9-2011

Spectral geometry image: Image based 3D models for digital broadcasting applications

Boon Seng CHEW
Nanyang Technological University

Lap Pui CHAU
Nanyang Technological University

Ying HE
Nanyang Technological University

Dayong WANG
Nanyang Technological University

Steven C. H. HOI
Singapore Management University, CHHOI@smu.edu.sg

DOI: https://doi.org/10.1109/TBC.2011.2151590

Published in IEEE Transactions on BroadcastingVolume 57, Issue 3, September 2011, Article number 5873171, Pages 636-645
https://doi.org/10.1109/TBC.2011.2151590

Spectral Geometry Image: Image Based 3D Models for Digital Broadcasting Applications

Boon-Seng Chew, Lap-Pui Chau, *Senior Member, IEEE*, Ying He, Dayong Wang, and Steven C. H. Hoi

***Abstract*—The use of 3D models for progressive transmission and broadcasting applications is an interesting challenge due to the nature and complexity of such content. In this paper, a new image format for the representation of 3D progressive model is proposed. The powerful spectral analysis is combined with the state of art Geometry Image(GI) to encode static 3D models into spectral geometry images(SGI) for robust 3D shape representation. Based on the 3D model's surface characteristics, SGI separated the geometrical image into low and high frequency layers to achieve effective Level of Details(LOD) modeling. For SGI, the connectivity data of the model is implicitly encoded in the image, thus removing the need for additional channel bits allocated for its protection during transmission. We demonstrated that by coupling SGI together with an efficient channel allocation scheme, an image based method for 3D representation suitable for adoption in conventional broadcasting standard is proposed. The proposed framework is effective in ensuring the smooth degradation of progressive 3D models across varying channel bandwidths and packet loss conditions.**

***Index Terms*—Broadcasting 3D contents, conformal parameterization, error resilience, geometry image, spectral analysis.**

I. Introduction

THE revolution of 3D-TV technology brings experiences of user's interaction with their conventional image, video and 3D graphical contents to a new dimension. The successful showing of digital movies such as 3D Avatar demonstrated the huge demand for 3D visualization across diversified viewers. Recently, several researches have been undertaken to address the challenges faced for the representation, storage and delivery for such content. We refer the readers to [1] for the state-of-art reviews in 3D video representation and storage. The broadcasting and distribution of stereoscopic images to static and mobile user was addressed in [2]. Reference [3] discussed the challenges faced for automatic conversion of 2D to 3D videos.

There is a distinct difference between 3D video content and 3D graphical models with the latter having the attribute of interactivity. The deployment of mobile broadcasting technology [4] such as Digital Video Broadcasting-Handheld(DVB-H), Digital Multimedia Broadcasting(DMB) and MediaFLO supports the delivery of multimedia contents across mobile and portable devices such as cell phones and PDAs. Reference [5] uses the MPEG-4 system to synthesize audio, 3D graphics, video, image and text content into a single content stream for interactive multimedia playback. However, although the MPEG-4 Binary format for Scene(BIFs) which is supported in T-DMB provides a general representation for 3D model, there are limitations for the progressive delivery of 3D graphics across the broadcasting network due to the complexity and data representation in 3D.

Conventionally, 3D models are represented using polygonal or triangular meshes. However, there are still limitations (1) dependency between layers (2) the need for additional channel protection for mesh connectivity information, for such representation during the encoding and transmission process. Geometry image is an effective solution for compressing shapes that are parameterized to the regular domain, like the rectangle or sphere [6]. Peyré and Mallat presented geometric bandlets to compress geometrically regular objects (like geometry images and normal maps) [7]. They showed that bandeletization algorithm removes the geometric redundancy of orthogonal wavelet coefficients and thus is more effective than the wavelet based compression. Lin *et al.* considered the use of JPEG2K for compression and delivery of a geometry image [8]. They made use of the ROI (region of interest) characteristic in JPEG2K to achieve view dependent streaming. However, the impact of channel loss towards the decodable bit-stream of the 3D geometry model was not discussed in [8].

Spectral geometry processing relies on the eigenvalues and eigenvectors from mesh operators to carry out desired tasks. Motivated by the similarity of the eigenvectors of the graph Laplacian and the discrete Fourier transform, Taubin reduced the surface smoothing problem to low-pass filtering of the discrete surface signals [9]. Since then, there are a large amount of work in spectral geometry processing. We refer the readers to the State of The Art Report (STAR) by Zhang *et al.* [10] for the most recent survey.

Lévy pointed out the eigenfunctions of the Laplace–Beltrami differential operator capture the global properties of the surface, in some sense, "understand" the geometry [11]. Vallet and Lévy derived a symmetric discrete Laplacians using discrete exterior calculus which guarantees the eigenfunctions form an orthonormal basis, called manifold harmonics basis, with positive eigenvalues [12]. They also developed an efficient and numerically stable approach to compute the eigenfunctions of the Laplacian for meshes with up to a million vertices.

Manifold harmonics provide a natural way to analyze the signals defined on surfaces of arbitrary topology in a Fourier-transform like fashion, which thus has a wide range of applications in geometry processing. Rustamov presented the Global Point Signature (GPS), a deformation invariant shape signature using

B.-S. Chew and L.-P. Chau are with the School of Electrical and Electronics Engineering, Nanyang Technological University, 639798 Singapore.

Y. He, D. Wang, and S. C. H. Hoi are with the School of Computer Engineering, Nanyang Technological University, 639798 Singapore.

the eigenvalues and eigenfunctions of the Laplace–Beltrami operator [13]. Rong *et al.* [14] proposed spectral mesh deformation that compactly encodes the deformation functions in the frequency domain. Liu *et al.* presented a robust, blind, and imperceptible spectral watermarking approach for polygonal meshes using manifold harmonics transform [15]. They demonstrated that the spectral approach is very promising to be robust against noise-addition and simplification attacks.

Another related work is the spectral coding algorithm presented by Karni and Gotsman [16]. First, it partitions the 3D model into several submeshes, then computes the spectral of the adjacency matrix for each submesh, and finally, quantizes the spectral coefficients to finite precision. Our spectral geometry image approach is different from [16] in that we partition the frequency domain into hierarchical layers, i.e., the base layer contains the smoothest geometry and the top layer contains the high frequency geometric details, and compress each layer with different compression rates. Furthermore, by taking advantage of the regular structure of geometry image, we can apply more advanced compression techniques (like JPEG2K) than the simple quantization used in [16]. Thus, our approach is more flexible and can achieve better compression ratio with less artifacts.

The other challenge in the work lies in the use of suitable channel protection scheme to ensure the efficient transmission of 3D information across erratic networks. Previously, unequal error protection scheme for image and wireless broadcast video content is proposed by Lei [17] and Wang [18] respectively. Recently, Bici *et al.* [19] and Alregib *et al.* [20] considered the direct delivery of 3D models using mesh based transmission taking into account both source and channel rate. Multiple description coding (MDC) [21], [22] forms the other class of error transmission scheme used for error resilient transmission aside Unequal Error Protection (UEP). In the MDC scheme, descriptions are generated from the sub-meshes of a single model, each containing the full connectivity information to increase the decodability of the model. Aside from the conventional schemes, Mondet *et al.* [23] proposed the progressive representations for streaming plant type models using retransmission scheme for lost packets. In [24], [25], Cheng *et al.* proposed a progressive transmission scheme based on an analytical model to investigate the progressive reconstruction of meshes across lossy channel. Li *et al.* [26] proposed a novel concept of generic middleware for handling different type of triangle based progressively compressed 3D models suited for efficient network delivery of 3D progressive mesh models. Lastly, Yang *et al.* [27] proposed an optimized scheme to jointly consider the texture effects and mesh representation based on rate-distortion surface to facilitate progressive transmission of 3D model with its respective texture information.

Our work differs from the mentioned literatures, we proposed a new concept spectral geometry image(SGI) and developed a framework to deliver progressively encoded 3D models using image approach suitable for broadcasting application. The preliminaries results were presented in [28]. We combined the use of spectral analysis with the state of art Geometry Image(GI) to encode static 3D models into SGI for robust 3D shape representation. SGI separated the geometrical image into low and high frequency layers based on the 3D model's surface characteristics to achieve effective Level of Details(LOD) modeling. Our experiment demonstrates that in term of flexibility and data size representation, the proposed SGI is more powerful compared to the conventional geometry image. In order to address the issue of transmission resilience for the delivery of SGI encoded images across lossy channels. An optimized joint source and channel coding framework is proposed to achieve optimal allocation of both source and channel bits. Finally, the experimental result shows that the proposed system is efficient in ensuring the graceful degradation of SGI data across different bit rates and varying channel conditions. As a summary, the contributions of this paper are as follow:

1) Propose a new concept of Spectral Geometry Image (SGI) and develop a framework of constructing spectral geometry images of real-world 3D models.
2) Show that spectral geometry image is more powerful and flexible than the conventional geometry images for 3D shape representation and compression.
3) Present a novel 3D transmission framework based on image representation of 3D model suitable for adoption in conventional broadcasting standard.

The remaining of the paper is organized as follow: Section II details the algorithm to construct spectral geometry image. Next, Section III discuss the challenges in data transmission across lossy channels and Section IV details the proposed Joint Source and Channel method for the SGI representation to address such problem. The experimental results of the proposed system are presented in Section V. Finally, we provide the conclusion to the paper in Section VI.

II. Geometry Encoding

The following sections present the algorithmic details of constructing spectral geometry image.

A. Manifold Harmonics Transformation

This subsection briefly reviews the algorithm to compute the spectrum of Laplacian, i.e., manifold harmonics basis. More details can be found in [12]. Given a surface M represented by a triangular mesh $M = (V, E, F)$ where V, E, and F are the vertex, edge and face sets, the symmetric Laplace-Beltrami operators is defined as:

$$\begin{cases} \triangle_{ij} = 0 & \text{if} \{v_i, v_j\} \notin E \\ \triangle_{ij} = \frac{\cot\alpha + \cot\beta}{\sqrt{A_i A_j}} & \text{if} \{v_i, v_j\} \in E \\ \triangle_{ii} = -\sum_j \triangle_{ij} \end{cases} \tag{1}$$

where A_i and A_j are the areas of the two triangles that share the edge $\{v_i, v_j\}$ and α and β are the two angles opposite to that edge. The eigenfunctions and eigenvalues of the Laplace-Beltrami operator are all the pairs (H^k, λ_k) that satisfy:

$$\triangle H^k = \lambda_k H^k. \tag{2}$$

Since the Laplacian $\triangle$ is a symmetric matrix, its eigenvalues are real and eigenfunctions are orthogonal. We sort the eigenvalues in the increasing order, $0 = \lambda_0 \leq \lambda_1 \leq \lambda_2 \cdots \leq \lambda_n$. These eigenfunctions are the basis functions and any scalar function defined on M can be projected onto them.

For each vertex v_i, define a hat function $\Phi_i : M \to \mathbb{R}$ such that $\Phi_i(v_i) = 1$ and $\Phi_i(v_j) = 0$ for all $j \neq i$. Then, the geometry of M is represented by functions $x = \sum_i x_i \Phi_i$ (resp. y, z),

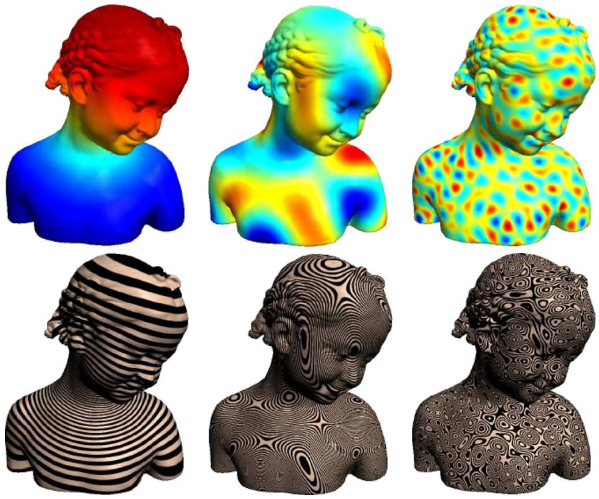

Fig. 1. Spectral analysis on 3D surface. The eigenfunctions of Laplace–Beltrami operator are orthogonal and serve the manifold harmonics basis. Row 1: The color indicates the function value. Row 2: The texture mapping shows the isocurves of the basis functions.

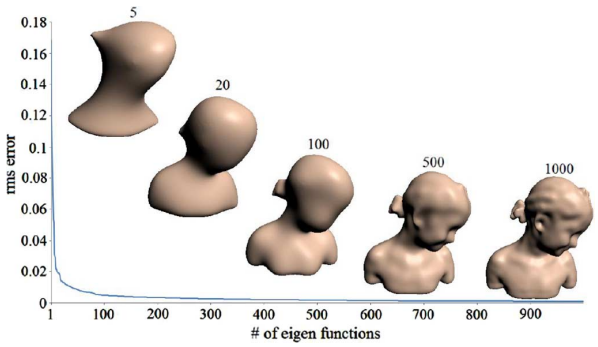

Fig. 2. Reconstructing the 3D mesh from the frequency domain. The number above each model is the number of eigenfunctions used in surface reconstruction.

where x_i denotes the x-coordinate of v_i. The eigenfunctions H^k can be represented as $H^k = \sum_i H_i^k \Phi_i$. Projecting the function x to manifold harmonics basis, we have

$$\tilde{x}_k = \langle x, H^k \rangle = \sum_i x_i H_i^k. \tag{3}$$

$\tilde{x}_k$ is the coefficient of k-th frequency of function x. Similarly, we can compute $\tilde{y}_k$ and $\tilde{z}_k$ for functions y and z, respectively.

To reconstruct the shape from the frequency domain, the coordinates of the vertex v_i are given by

$$x_i = \sum_{k=1}^{m} \tilde{x}_k H_i^k, y_i = \sum_{k=1}^{m} \tilde{y}_k H_i^k, z_i = \sum_{k=1}^{m} \tilde{z}_k H_i^k, \tag{4}$$

where m is the user-specified number of eigenfunctions. With the increasing number of eigenfunctions, the shape can be faithfully reconstructed from the frequency domain. Figs. 1 and 2 illustrate the manifold harmonics transformation on the Bimba model.

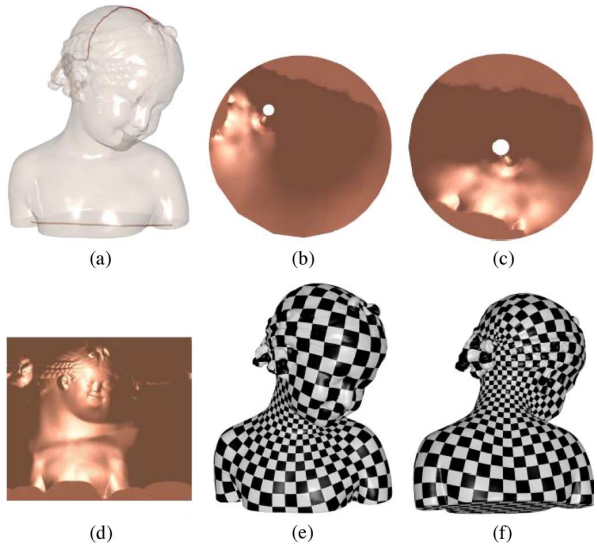

Fig. 3. Conformal parameterization of the genus-0 Bimba model. (a) We first modify its topology by two cuts: one at the top and the other at the bottom of the model. The cut surface M' is a topological cylinder. (b) Then, we compute the uniform flat metric by discrete Ricci flow and embed M' to a topological annulus. (c) Next, we map the topological annulus to a canonical annulus by a Möbius transformation. (d) We cut the canonical annulus by a line passing through the origin and conformally map it to a rectangle. (e)–(f) The checkerboard texture mapping illustrates the conformality of the parameterization.

B. Conformal Parameterizations of 3D Models to Rectangular Domain

A key step in constructing (spectral) geometry image is to parameterize the 3D model M to a rectangular domain $D \in \mathbb{R}^2$. Although there are many surface parameterizations techniques, we prefer the conformal parameterization (see Fig. 3)<<AQ1>> due to its shape preserving property and numerical stability [29]. In this paper, we focus on the genus-0 closed surface.

Topological Modification:: We first modify its topology by two cuts, i.e., one at the top and the other at the bottom of M. Let M' denote the resultant open surface. Note that M' has the same geometry of M, but is a topological cylinder.

Computing the Uniform Flat Metric:: Let g denote the Riemannian metric of M'. We want to compute a metric that is conformal to g and flat everywhere inside M' and the geodesic curvature is constant on the boundary $\partial M'$. Such a metric is called uniform flat metric. It is proven that if the total geodesic curvature on each boundary is given, such a uniform flat metric exists and is unique.

In our implementation, we use discrete Ricci flow [30] to compute the uniform flat metric. We set the target Gaussian curvature of each interior point to zero, i.e., it is completely flat, $\bar{K} = 0, v \notin \partial M'$. M' has two boundaries, $\partial M' = C_0 \cup C_1$, where C_0 is the boundary with the longer length. Then we set the total geodesic curvature of the boundary C_0 and C_1 to be 2π and -2π respectively, i.e., $\int_{C_0} \bar{k} = 2\pi$ and $\int_{C_1} \bar{k} = -2\pi$. It can be easily verified that the total geodesic and Gaussian curvatures satisfy the Gauss-Bonnet theorem,

$$\int_{M'} K + \int_{\partial M'} k = \int_{M'} \bar{K} + \int_{\partial M'} \bar{k} = 2\pi\chi, \tag{5}$$

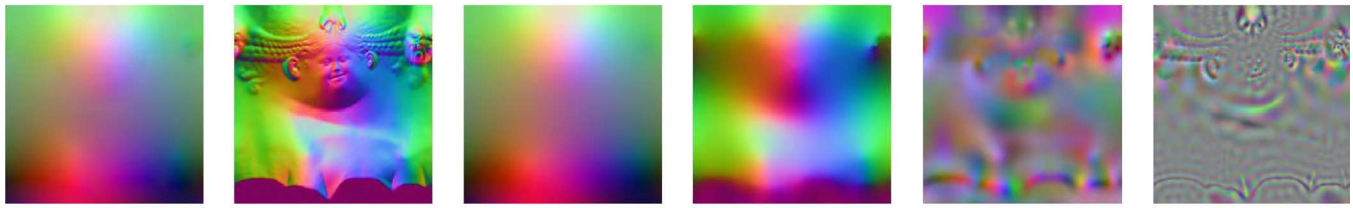

(a) (b) (c) (d) (e) (f)

Fig. 4. Spectral geometry image. (a)–(b) The geometry image of the Bimba model. (c)–(f) The three-layer spectral geometry image. The normal maps in (b) and (d) highlight the difference between SGI_1 and GI. To better view the high frequency layers (e) SGI_2 and (f) SGI_3, the pixel values are normalized to [0,255].

where $\chi = 0$ is the Euler number of M'. It is proven that discrete Ricci flow converges exponentially fast [31] and the steady state is the desired uniform flat metric. With the uniform flat metric, the Gaussian curvature of interior vertices are zero, thus, the faces can be flattened one by one on the plane.

Conformal Map to a Canonical Annulus:: Note that the embedded surface $\phi(M')$ may not be the canonical annulus. Let $\phi(C_1) : |z - c_1| = r_1$ and $\phi(C_2) : |z - c_2| = r_2$ be the outer and inner circles of the topological annulus. We want to find a Möbius transformation $w : \mathbb{C} \to \mathbb{C}$ to map $\phi(C_1)$ and $\phi(C_2)$ to concentric circles with center at the origin. A Möbius transformation is uniquely determined by three pairs of distinct vertices $z_i \in \mathbb{C}$ and $w_i \in \mathbb{C}$, $i = 1, 2, 3$, such that $w(z_i) = w_i$. Set $w_1 = 0$ and $w_2 = \infty$, i.e., w_1 and w_2 are symmetric w.r.t. the canonical annulus. Therefore, the pre-images z_1 and z_2 are symmetric w.r.t. $\phi(C_1)$ and $\phi(C_2)$, i.e., $|z_1 - c_1||z_2 - c_1| = r_1^2$ and $|z_1 - c_2||z_2 - c_2| = r_2^2$. We also set $z_3 = c_1 + (r_1, 0)$ and $|w_3| = 1$, i.e., the radius of the outer circle in the canonical annulus is one. Then, the Möbius transformation is given by

$$w(z) = \rho e^{i\theta} \frac{z - z_1}{z - z_2}, \tag{6}$$

where $\rho = |z_3 - z_2|/|z_3 - z_1|$ and θ is an arbitrary angle.

Conformal Map to a Rectangular Domain:: We cut the canonical annulus by a line passing through (0,0) and (1,0). Finally, we conformally map the cut annulus to a rectangular domain by

$$\psi(z) = |z| + i \arg z, \qquad z \in \mathbb{C} \tag{7}$$

Putting them all together, the conformal parameterization $f : M' \to D \in \mathbb{R}^2$ is given by the composite map, which is guaranteed to be conformal (angle-preserving) and diffeomorphism.

$$f = \psi \circ w \circ \phi, \tag{8}$$

where $\circ$ denotes function composition. The checkerboard texture mapping illustrates the conformality of the parameterizations.

C. Construction of Spectral Geometry Image

Spectral geometry image is more flexible than the conventional geometry image due to its capability to separate geometry image into low- and high-frequency layers. Note that the low-frequency layers represent the rough shape and the high-frequency layers represent the detailed geometry. In our framework, the user specifies the number of desired layers l and the reconstruction tolerance for each layer ϵ_i, $i = 1, \cdots, l-1$. We denote M_i the reconstructed mesh with m_i eigenfunctions where m_i is determined by finding the smallest integer such that

$$\|M_i - M\|_\infty = \max_j \sqrt{\sum_{k=m_i+1}^{\infty} \left(\tilde{x}_k H_j^k\right)^2 + \left(\tilde{y}_k H_j^k\right)^2 + \left(\tilde{z}_k H_j^k\right)^2} \leq \epsilon_i$$

The spectral geometry images are defined as follows:

$$SGI_i : M_i - M_{i-1} \to D, \forall i \tag{9}$$

Intuitively speaking, M_1 represents the coarsest reconstruction of the 3D model. The remaining layers M_i encode the displacement between the following two consecutive layers M_i and M_{i-1} and present the model with increasing quality until the original model is decoded in the top layer M_l. Thus, to reconstruct the geometry with the user-specified tolerance ϵ_i, we simply add the layers up to i. Fig. 4 shows the 3-layer spectral geometry image of the Bimba model with the tolerances $\epsilon_1 = 0.04$ and $\epsilon_2 = 0.01$. The model is normalized to a unit cube.

III. Channel Coding

The Reed-Solomon (RS) code is used as the error control code to provide the SGI encoded image with some measure of reliability during the transmission across lossy communication channel. Typically, it can be described as an (n,k,t) code. The code block length n is limited by $n \leq 2^m - 1$ where m is the numbers of bits per symbol. The codeblock contains $k = n - 2t$ source symbols defined by the Galois fields over GF(2^8). RS is a well known class of block codes among FEC that provides good erasure correction properties and is commonly used in storage devices for the correction of burst errors. Here, an (n,k,t) codes will be able to correct up to 2t (protection symbol) or t errors where each error is taken as two erasures.

A. Channel Model

The network often plays a crucial role in the resultant reconstructed quality of the 3D model upon transmission. However, the process of determining the individual packet behavior over a real-time channel is often complex in nature. In this paper, we assume the existence of a channel estimator to simulate such characteristic. The two state Markovian Gilbert-Elliot model is used in the paper. State 0 is denoted as a packet being correctly received and state 1 indicates a lost packet. P(1|0) and P(0|1) fully described the transitional probabilities between the two

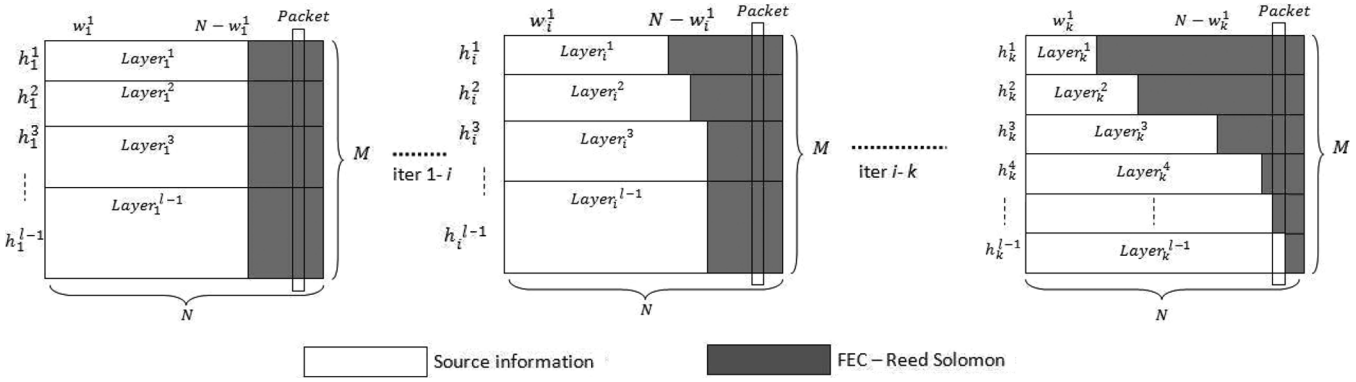

Fig. 5. Packetization scheme. The figure demonstrates the packetization scheme and UEP allocation adopted for the SGI encoded model from the initial EEP configuration.

states. To make the parameters more intuitive in nature, the average loss probability $P_{loss} = P(1|0)/P(1|0) + P(0|1)$ and average burst length $L = 1/P(0|1)$ are used in the simulation.

B. Problem Formulation

In this section, we discussed the allocation problem for both source and channel bits given the input of varying bandwidth limitations and channel loss characteristics. For the purpose of progressive transmission, the input spectral geometry image is decomposed into l image layers to support the reconstruction of partial bit-stream from coarse to high quality 3D models at the decoder. However, due to the dependency between the layers of such multi-resolution model, the effects of channel error on the decoded 3D model can be extremely significant during transmission. Thus, there is a need to exert some form of error control to ensure a measure of reliability is maintained in the presence of such error. The forward error code aims to protect data against channel errors through the introduction of parity codes. However, in a conventional transmission system where bandwidth is limited, there is often a dilemma in resource allocation between the source and channel blocks where better quality encoding needs to be balanced against having sufficient channel protection. In this paper, the joint source-channel coding system for SGI representation is considered. The proposed scheme mitigates the problem of resource allocation for both source and channel bits to achieve an overall improved 3D model quality with SGI upon transmission.

IV. JSCC FOR SGI

Let the set of channel code rate for the individual SGI layers be denoted as $C = \{C_1, C_2, \ldots C_{l-1}\}$ where $C_1 \geq C_2 \geq , \ldots, \geq C_{l-1}$. The channel rate follows the pattern of non-decreasing to take into consideration importance of the different SGI layers. That is, more channel information in the form of RS code will be assigned to the higher priority lower layers as compared to the higher layers which contain the finer details of the model. The total bit budget, Q_{budget} defines the maximum bandwidth available during the transmission. Given an overall coding rate of R_{s+c} for SGI source coding and RS codes, the objective is to optimally allocates bits such that the total distortion D_{s+c} is minimized, that is,

$$\min D_{s+c}, \text{ subjected to } R_{s+c} \leq Q_{budget} \tag{10}$$

Out of consideration for data packetization before the progressive 3D model transmission, we denote the width and height of different layers of SGI bitstreams as w^j and h^j respectively. Here, j represent the layers number where $j = 1, 2, \ldots, l-1$. The packet number and packet size is denoted by N and M respectively. The packetization scheme is illustrated in Fig. 5. In order to prevent the lost of consecutive packets containing correlated information when burst errors occur, the allocation of FEC is done horizontally and the packets are vertically packed. For the ith layer, with length K^i, we denote the width w^i for the individual layer using the following equation:

$$w^i = \beta^i / K^i + \alpha \tag{11}$$

where β^i represents the data size (bytes) for layer i. In the case whereby division of β^i/K^i holds no remainders, $\alpha = 0$ or $\alpha = 1$. The remaining space of the bounding area of $K^i \times w^i$ will be filled up with data from the next layer. Finally, the packet size will be limited by the following constraint:

$$\sum_{j=1}^{l-1} h^j \leq M \tag{12}$$

We denote the probability of recovering the i layer as $P_i \in i = 1, \ldots, l-1$. Let $\lambda = D_1 P_1$, λ shows the initial distortion obtained from decoding the base layer upon transmission. The resultant distortion from the remaining layers $D_{s+c}(k)$ can now be easily determined through the following equations:

$$\varepsilon_{i,k} = \Sigma_{i=1}^{N-w} D_{i,k}(P_{i,k|C_k}) \tag{13}$$

Here, $D_{s+c}(k) = \lambda + \varepsilon_{i,k}\xi_k$, if $1 \leq k \leq l-1$ and $D_{s+c}(k) = \lambda + \varepsilon_{i,k-1}\xi_{k-1} + D_k\xi_k$, if $k = l$, where $\xi_j = \prod_{i=0}^{j-1}(1 - P_i)$. For the computation of the packet loss probability, $P(m, n)$, let n be the total packets transmitted across the channel and m is the number of packets lost during the process. For layered i, where RS codes is applied for packet error protection. $P_i = \Sigma_{m=0}^{N-w} P(m, n)$ denotes the probability that ith SGI layer is decodable. For experimental purpose, the earlier discussed two-state Markov model is used to simulate the lossy nature of the erratic channel. Fig. 6 denotes the packet error probability for the varying channel loss rate.

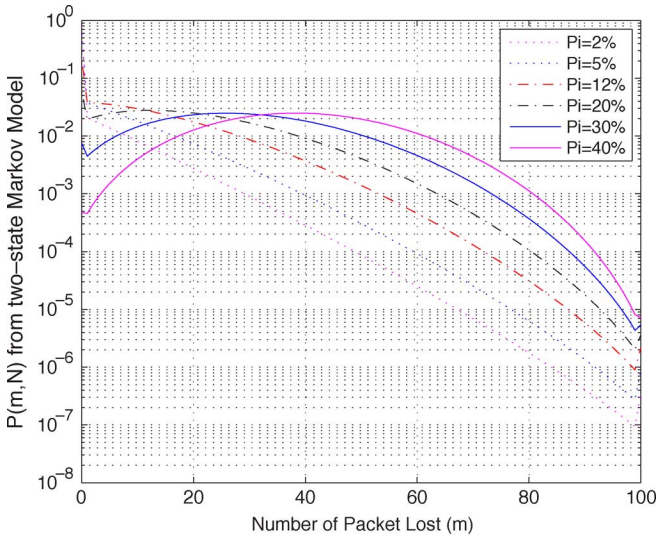

Fig. 6. Packet loss probability, P(m,n). Block length $\mathrm{N} = 100$, $B_L = 9.57$ and $\mathrm{Pi} = 2\%$, 5%, 12%, 20% ,30% and 40% respectively.

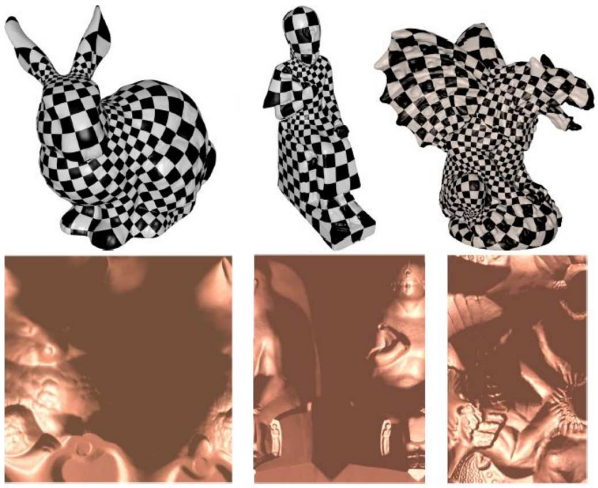

(a) (b) (c)

Fig. 7. Conformal parameterization of the test models. (a) Bunny. (b) Ramesses. (c) Gargoyle.

A. Distortion Metric

To measure the quality of the compressed surface M', we use the d_H [16] based on the average of norm of geometric and Laplacian differences to determine the model's quality.

$$d_H(M, M') = \frac{1}{2}\left(d_r + \sqrt{\frac{1}{|V|}\sum_{i=1}^{|V|} ||L(v_i) - L\left(v_i'\right)||^2} \right) \tag{14}$$

$|V|$ is the number of vertices in M and M'. Note that $L(v_i)$ denote the geometric Laplacian for vertex v_i. d_H measures the smoothness of the compressed mesh through the calculation of Laplacian operator and is able to reflect the visual quality better compared to Euclidean measurement such as Root Mean Square (RMS) which only consider the geometric distance.

Fig. 7 shows the test models and their parameterizations and Fig. 8 compares the performance of GI and SGI of the Bunny model. We use d_H to measure the smoothness of the compressed

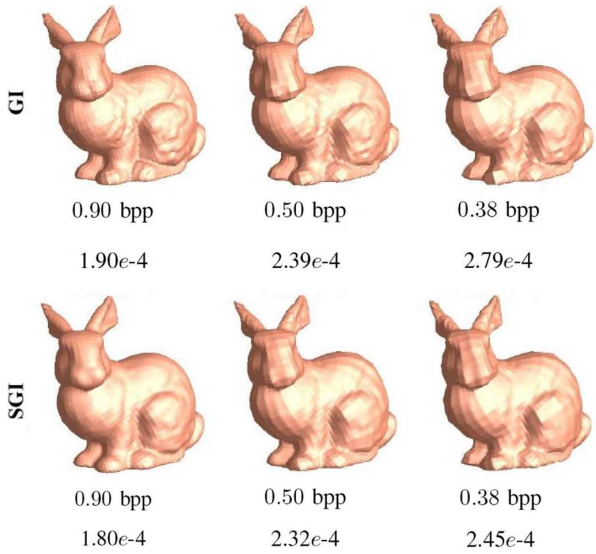

Fig. 8. Mean curvature error d_H measures the visual quality. Row 1: The GI of resolution 256 × 256; Row 2: the three-layer SGI of resolution 64 × 64, 128 × 128 and 256 × 256. The numbers below each figure are the *bits per pixel (bpp)* and the mean curvature error d_H. SGI has smaller d_H at low bpp because the high-frequency layer is discarded and the low-frequency layer has less distortion than GI.

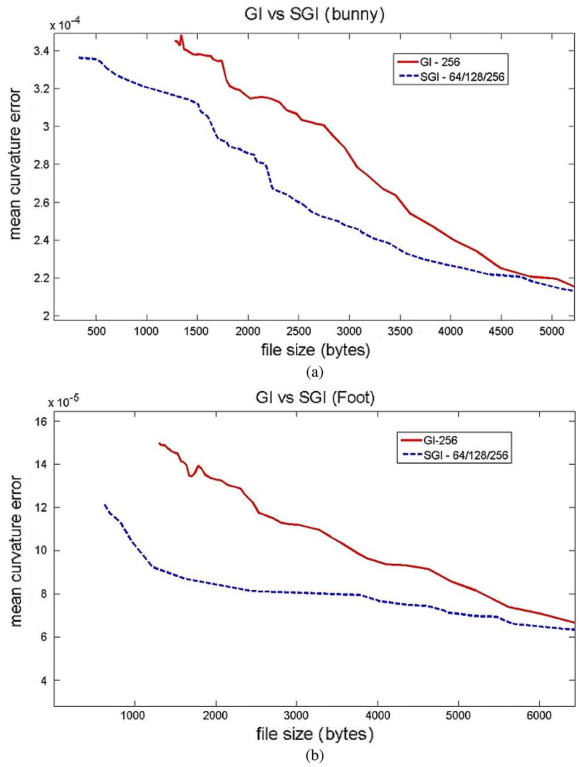

Fig. 9. Shape compression using geometry image (GI) and spectral geometry image (SGI). GI is of resolution 256 × 256 for both models. We constructed two SGIs with 3 layers respectively . Both Bunny and Foot models are of resolution 64 × 64, 128 × 128, and 256 × 256. As shown in (a) and (b), SGI's performance is better than GI for varying compression rates.

models. Note that both GI and SGI discard high frequency details at high compression rate. The low-frequency layer of SGI is more smooth than that of GI and thus lead to less artifacts. Fig. 9 compares the performance of GI and SGI of the Bunny

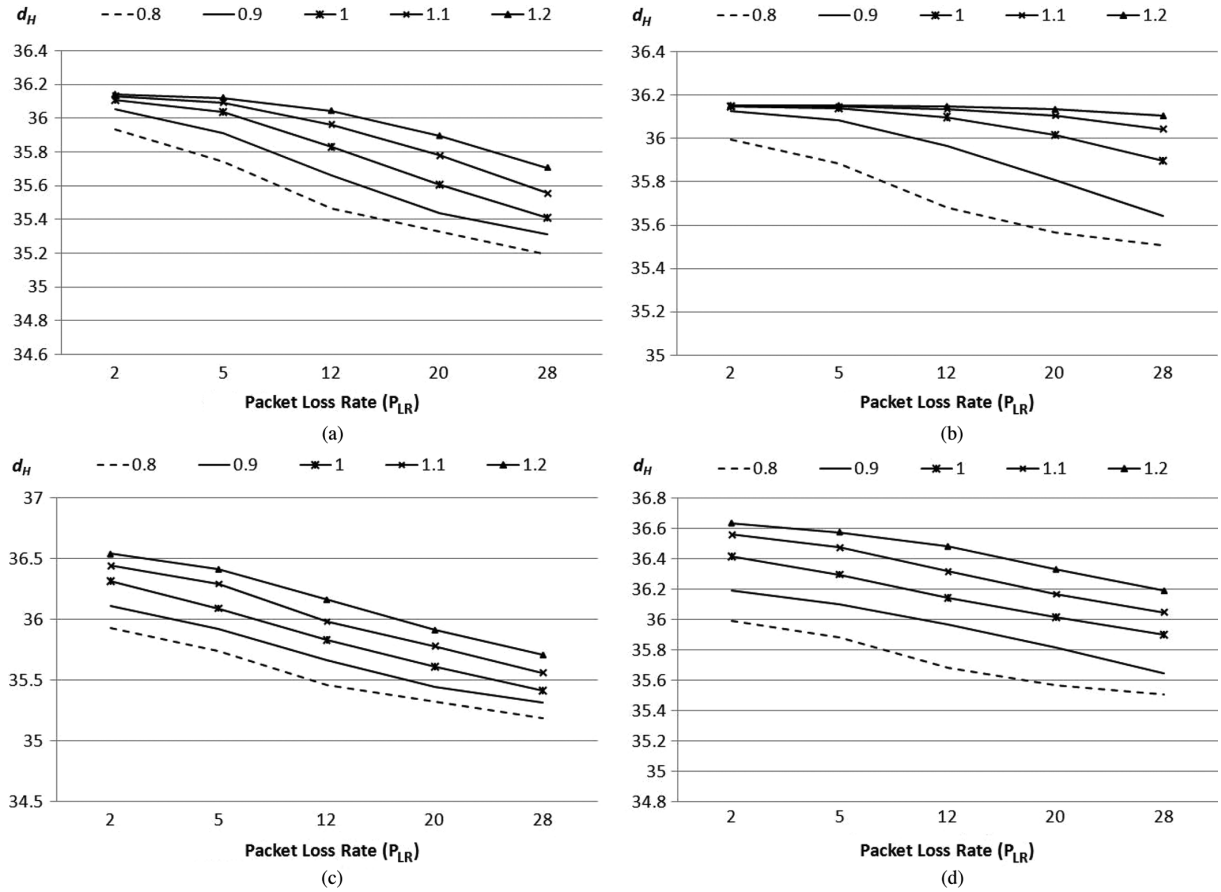

Fig. 10. Comparison of error protection schemes. (a)–(b) The mean curvature error for both (a) EEP and (b) UEP scheme with fixed source rate of 0.8 bpp and 0.1–0.4 bpp channel rate for the Bunny model. (c)–(d) The mean curvature error for both (c) optimized EEP and (d)JSCC scheme with overall bit rate of 0.8–1.2 bpp for the Bunny model. Horizontal axis denote the packet lost rate P_{LR} in (%). The mean curvature error d_H is represented by $10log_{10}1/d_H$.

and Foot model. When reconstructing the geometry from multi-layer SGI of different resolutions, we up-sample the bottom layers to the resolution of the top-most layers. This upsampling usually smoothes the low-frequency geometry, but it does not change the top-most layer that contains the high-frequency details within the user-specified range. Since the Laplacian operator encodes the differential coordinates [16] representing the local details, it is insensitive towards the small-scale deformation of the bottom layers. As a result, the SGI-64/128/256 outperforms the GI-256 in terms of mean curvature error. In this paper, the visual metric d_H is used to determine the contribution from each source layer of the compressed model. Although other form of Euclidean error measurements such as Hausdorff distance or root mean square rms can be used, d_H which measure the smoothness of the surface of a model, can better reflect the visual quality of a compressed model in term of error.

V. Simulation Results

A distortion optimal rate allocation algorithm is proposed to provide the SGI encoded model with efficient channel protection during transmission. In our experiment, we simulate the bitstream over packet loss channel using a two-state Markovian model as the channel estimator. The average block length B_L is set as 9.57 and the channel loss rate was determined using Gaussian distribution over 100 cycles for 2%, 5%, 12%, 20% and 28% to simulate the randomness in a broadcast channel. In consideration for the source coding rate of the 3D model, we select a subset of $C_r = (5, 10, \ldots 300)$, where C_r denote the compression rate, for the i layered of SGI image encode using J2K standard to ease the computation in the simulation. We use the Bunny (SGI-64/128/256) and Foot (SGI-64/128/256) to show our experiment results. The source bit rate and overall bit rate are 0.8bpp and 0.8-1.2 bpp for the Bunny model, 1.2 bpp and 1.2–1.6 bpp for the Foot model in both EEP and UEP setting. We illustrated the performance (d_H) over the range of average packet error loss rate P_{LR} in Figs. 10 and 11. For each experiment, the results from our proposed JSCC algorithm are compared against the performances of the following schemes. Figs. 10(a) and 11(a) depict the results for the EEP method where EEP assigns equal channel rates to each SGI encoded layers respectively without considering the importance of the layer. The simulation results using the UEP method is presented in Figs. 10(b) and 11(b). For UEP, unequal channel rates are allocated to the SGI layers based on their layer importance. Since the SGI is constructed based on the frequency components of the 3D model, the lower layers which contain the rough shape of the original model carries the more essential information to be protected during transmission. Figs. 10(c) and 11(c) shows the results from the optimized EEP scheme. The overall bit rate is 1.2 bpp and 1.6 bpp for the bunny and Foot model. Unlike the

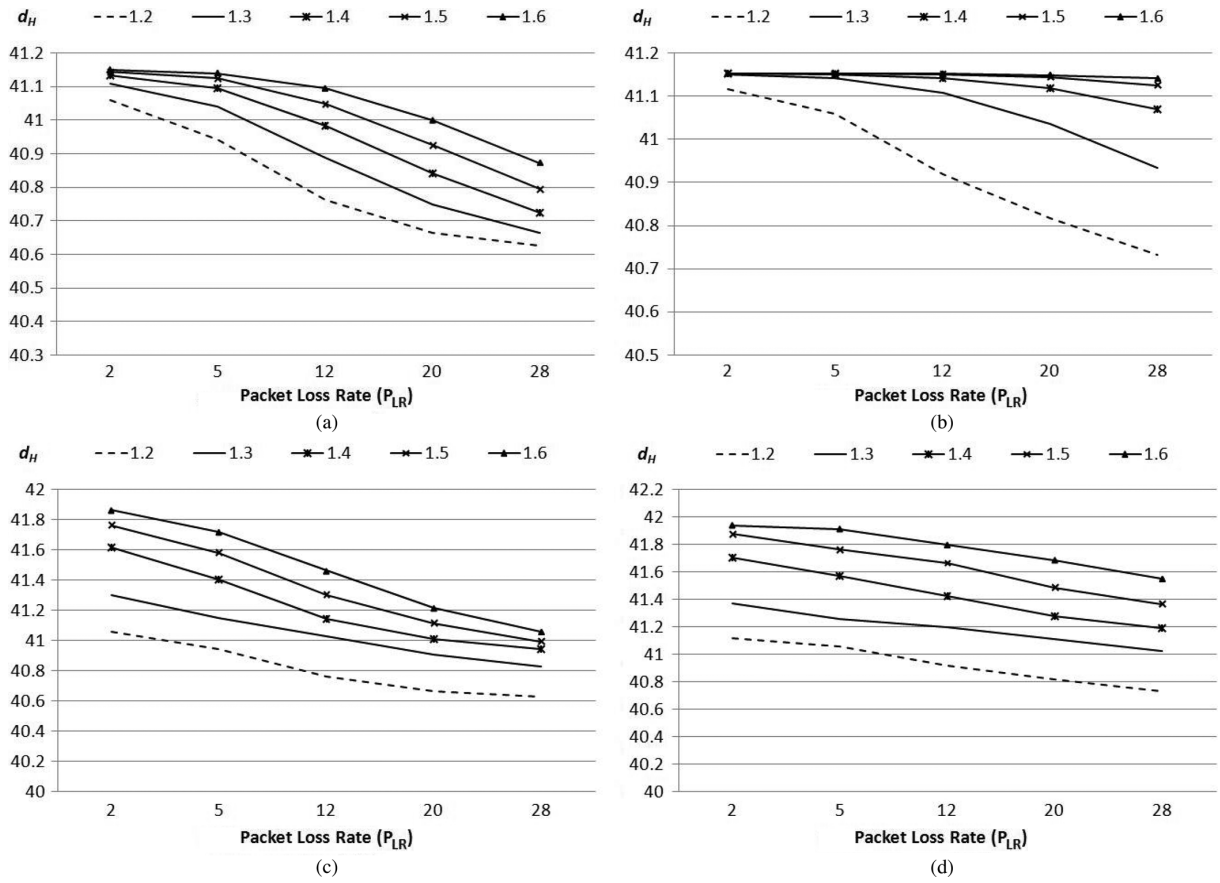

Fig. 11. Comparison of error protection schemes. (a)–(b) The mean curvature error for both (a) EEP and (b) UEP scheme with fixed source rate of 1.2 bpp and 0.1–0.4 bpp channel rate for the Foot model. (c)–(d) The mean curvature error for both (c) optimized EEP and (d) JSCC scheme with overall bit rate of 1.2–1.6 bpp for the Foot model. Horizontal axis denote the packet lost rate P_{LR} in (%). The mean curvature error d_H is represented by $10log_{10}1/d_H$.

earlier EEP scheme where the source bit rate is fixed, the optimized EEP method determined the best source and channel bit rate set and assigned channel bits equally across all layers.

It is important to note that our proposed scheme differs from the conventional transmission methods. For SGI, the 3D static model is first encoded into multiple images of difference importance. Unlike conventional methods for 3D model transmission, the connectivity information of the 3D model is implicitly encoded within the SGI, thus there isn't a need for additional protection to ensure the connectivity information lossless delivery. Secondly, the source and channel bits of the SGI layers are jointly optimized before transmission. In Figs. 10 and 11, we show that the proposed solution is able to provide a more graceful degradation of decoded model quality compared to the optimized EEP method and consistently shows a better decoded model quality against the other solutions across varying packet loss rate. From our observation, the proposed JSCC method outperforms the EEP, UEP and optimized EEP by a d_H of 0.678, 0.411 and 0.493 respectively for the overall bit rate of 1.6 bpp and (P_{LR}) of 28% for foot model. d_H denotes the mean curvature error represented by $10log_{10}1/d_H$. For the bunny model, the proposed JSCC method also shows an improvement of 0.1–0.48 d_H across the different methods. In the second experiment, we compared our proposed SGI scheme to the state-of-art GI technique applying similar JSCC technique to both methods for a fair comparison. Due to the efficient application of JSCC scheme for both SGI and GI method, both schemes show a smooth decrease in quality (d_H) during channel simulation across varying channel condition. Fig. 12 shows that the SGI is capable of ensuring a better quality 3D model decoded throughout the simulation. This is due to the efficient allocation of the lower frequency geometry of the SGI into the initial layers of the SGI encoded image. During the channel allocation, more channel bits will be allocated to the lower layers compared to the GI scheme, thus better resilience of the earlier layers can be ensured. Fig. 12 demonstrate the improvement of SGI over GI across varying channel condition.

VI. Conclusion

In this paper, an image based method for 3D representation suitable for adoption in conventional broadcasting standard is proposed. We investigated the problem of delivering progressively encoded 3D content across packet erasure channels. The paper introduce a novel 3D encoding method, Spectral Geometry Image(SGI), which is more robust, and efficient in comparison to the state of art Geometry Image technique for 3D models representation. We showed that by coupling SGI together with the proposed JSCC allocation scheme, an effective framework for delivery of progressively encoded 3D model is realized. Experimental results demonstrated this fact and showed that the

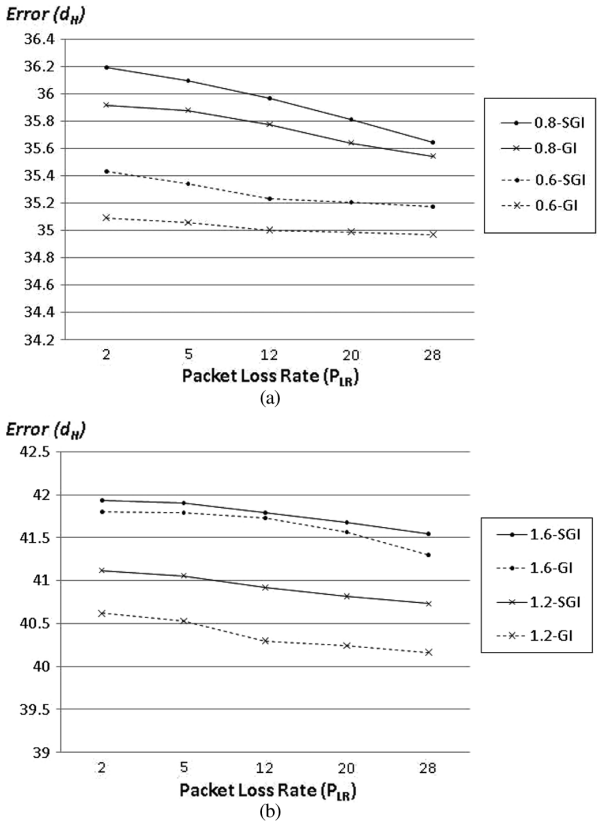

Fig. 12. Comparison of d_H between JSCC allocation scheme for both GI and SGI method. (a)–(b) The simulation results for (a) Bunny and (b) Foot model across varying packet loss rate. GI and SGI are both of resolution 256×256. As shown, SGI outperforms GI for various packet loss condition. The number below the figure are the packet lost rate (%) and the vertical axis is the d_H denoted in $(10log_{10}1/d_r)$.

proposed method outperform the conventional GI in term of coding efficiency and error resilience performance simulated for varying packet lost rates.

REFERENCES

[1] A. Vetro, A. M. Tourapis, K. Muller, and T. Chen, "3D-TV content storage and transmission," *IEEE Trans. Broadcast.*, Jun. 2011.

[2] N. Hur, H. Lee, G. S. Lee, S. J. Lee, A. Gotchev, and S.-I. Park, "3DTV broadcasting and distribution systems," *IEEE Trans. Broadcast.*, Jun. 2011.

[3] L. Zhang, C. Vazquez, and S. Knorr, "3D-TV content creation: Automatic 2d-to-3d video conversion," *IEEE Trans. Broadcast.*, Jun. 2011.

[4] F. Hartung, U. Horn, J. Huschke, M. Kampmann, T. Lohmar, and M. Lundevall, "Delivery of broadcast services in 3G networks," *IEEE Trans. Broadcast.*, vol. 53, no. 1, pp. 188–199, Mar. 2007.

[5] W.-S. Cheong, J. Cha, S. Ahn, W.-H. Yoo, and K. A. Moon, "Interactive terrestrial digital multimedia broadcasting(T-DMB) player," *IEEE Trans. Consum. Electron.*, vol. 53, no. 1, pp. 65–71, Feb. 2007.

[6] X. Gu, S. J. Gortler, and H. Hoppe, "Geometry images," *SIGGRAPH*, pp. 355–361, 2002.

[7] G. Peyré and S. Mallat, "Surface compression with geometric bandelets," in *Proc SIGGRAPH*, NY, 2005, pp. 601–608.

[8] N.-H. Lin, T.-H. Huang, and B.-Y. Chen, "3d model streaming based on jpeg 2000," *IEEE Trans. Consumer Electron.*, vol. 53, no. 1, pp. 182–190, Feb. 2007.

[9] G. Taubin, "A signal processing approach to fair surface design," in *SIGGRAPH*, 1995, pp. 351–358.

[10] H. Zhang, O. van Kaick, and R. Dyer, "Spectral methods for mesh processing and analysis," in *Proc. Eurographics State-of-the-Art Rep.*, 2007, pp. 1–22.

[11] B. Lévy, "Laplace-beltrami eigenfunctions towards an algorithm that "understands" geometry," *SMI*, p. 13, 2006.

[12] B. Vallet and B. Lévy, "Spectral geometry processing with manifold harmonics," *Comput. Graph. Forum*, vol. 27, no. 2, pp. 251–260, 2008.

[13] R. M. Rustamov, "Laplace-beltrami eigenfunctions for deformation invariant shape representation," in *Symp. Geometry Process.*, 2007, pp. 225–233.

[14] G. Rong, Y. Cao, and X. Guo, "Spectral mesh deformation," *The Visual Computer*, vol. 24, no. 7–9, pp. 787–796, 2008.

[15] Y. Liu, B. Prabhakaran, and X. Guo, "A robust spectral approach for blind watermarking of manifold surfaces," *MM&Sec*, pp. 43–52, 2008.

[16] Z. Karni and C. Gotsman, "Spectral compression of mesh geometry," in *Proc. SIGGRAPH*, 2000, pp. 279–286.

[17] L. Cao, "On the unequal error protection for progressive image transmission," *IEEE Trans. Image Process.*, vol. 16, no. 9, pp. 2384–2388, Sep. 2007.

[18] Y. Wang and L.-P. Chau, "Bit-rate allocation for broadcasting of scalable video over wireless network," *IEEE Trans. Broadcast.*, vol. 56, no. 3, pp. 288–295, Sep. 2010.

[19] M. Bici, A. Norkin, and G. Akar, "Packet loss resilient transmission of 3d models," in *Proc. IEEE Int. Conf. Image Processing, ICIP 2007*, Oct. 2007, pp. 121–124.

[20] G. Alregib, Y. Altunbasak, and J. Rossignac, "Error-resilient transmission of 3d models," *ACM Trans. Graph.*, vol. 24, no. 2, pp. 182–208, 2005.

[21] M. Bici and G. Akar, "Multiple description scalar quantization based 3d mesh coding," in *Proc. IEEE Int. Conf. Image Proc., ICIP*, Oct. 2006, pp. 553–556.

[22] M. Bici, A. Norkin, G. Akar, A. Gotchev, and J. Astola, "Multiple description coding of 3d geometry with forward error correction codes," in *Proc. of 3DTV Conf.*, May 2007, pp. 1–4.

[23] S. Mondet, W. Cheng, G. Morin, R. Grigoras, F. Boudon, and W. T. Ooi, "Streaming of plants in distributed virtual environments," in *Proc. ACM Multimedia*, NY, 2008, pp. 1–10.

[24] W. Cheng, "Streaming of 3d progressive meshes," in *Proc. ACM Multimedia*, NY, 2008, pp. 1047–1050.

[25] W. Cheng, W. T. Ooi, S. Mondet, R. Grigoras, and G. Morin, "An analytical model for progressive mesh streaming," in *Proc. ACM Multimedia*, NY, USA, 2007, pp. 737–746.

[26] H. Li, M. Li, and B. Prabhakaran, "Middleware for streaming 3d progressive meshes over lossy networks," *ACM Trans. Multimedia Comput. Commun. Appl.*, vol. 2, no. 4, pp. 282–317, 2006.

[27] S. Yang, C.-H. Lee, and C.-C. J. Kuo, "Optimized mesh and texture multiplexing for progressive textured model transmission," in *Proc. ACM Multimedia*, NY, 2004, pp. 676–683.

[28] Y. He, B. S. Chew, D. Wang, H. Steven, and L. P. Chau, "Streaming progressive 3d model using spectral geometry images," in *Proc. ACM Multimedia*, Oct. 2009, pp. 431–440.

[29] X. Gu and S.-T. Yau, "Global conformal parameterization," in *Symp. Geometry Processing*, 2003, pp. 127–137.

[30] X. Gu, S. Wang, J. Kim, Y. Zeng, Y. Wang, H. Qin, and D. Samaras, "Ricci flow for 3d shape analysis," in *ICCV*, 2007, pp. 1–8.

[31] B. Chow and F. Luo, "Combinatorial ricci flows on surfaces," *J. Differential Geom.*, vol. 63, no. 1, pp. 97–129, 2003.

Boon-Seng Chew received the B.Eng. degree in electrical and electronic engineering from Nanyang Technological University, Singapore, in 2005. He is currently pursuing the Ph.D. degree in information engineering from the School of Electrical and Electronics Engineering, Nanyang Technological University, Singapore. He joined Defence Science Technology Agency of Singapore (DSTA) in 2010 as a system engineer. His current research interests include 3D graphics/animation compression and transmission, signal processing and multimedia application.

Lap-Pui Chau (SM'03) received the B.Eng. degree with first class honors in electronic engineering from Oxford Brookes University, England, and the Ph.D. degree in electronic engineering from Hong Kong Polytechnic University, Hong Kong, in 1992 and 1997, respectively.

In June 1996, he joined Tritech Microelectronics as a Senior Engineer. Since March 1997, he joined School of Electrical & Electronic Engineering, Nanyang Technological University, Singapore as a research fellow, then assistant professor and currently, he is an Associate Professor. His research interests include streaming media, multimedia coding and compression, and VLSI for signal processing. He involved in organization committee of international conferences including the IEEE International Conference on Image Processing (ICIP 2010, ICIP 2004), and IEEE International Conference on Multimedia & Expo (ICME 2010). He is a Technical Program Co-Chair for 2010 International Symposium on Intelligent Signal Processing and Communications Systems (ISPACS 2010). Besides, he also served as track chairs in technical program committee for many international conferences regularly. He is a senior member of the IEEE, the Chair of Technical Committee on Circuits & Systems for Communications (TC-CASC), a member of Technical Committee on Multimedia Systems and Applications (TC-MSA) and Technical Committee on Visual Signal Processing and Communications (TC-VSPC) of IEEE Circuits and Systems Society. He was the chairman of IEEE Singapore Circuits and Systems Chapter from 2009 to 2010. He served as a member of Singapore Digital Television Technical Committee from 1998 to 1999. He served as an Associate Editor for IEEE TRANSACTIONS ON MULTIMEDIA, and is currently serving as an associate editor for IEEE Trans. Circuits and Systems for Video Technology, IEEE TRANSACTIONS ON BROADCASTING, IEEE SIGNAL PROCESSING LETTERS and IEEE TECHNOLOGY NEWS. Besides, he is IEEE Distinguished Lecturer for 2009–2013, and a steering committee member of IEEE TRANSACTIONS FOR MOBILE COMPUTING from 2011–2012.

Ying-He received the BS and MS degrees in electrical engineering from Tsinghua University, China, and the Ph.D. degree in computer science from the State University of New York (SUNY), Stony Brook.

He is currently an Assistant Professor at the School of Computer Engineering, Nanyang Technological University, Singapore. His research interests include computer graphics, computer-aided design, and scientific visualization. His major works include manifold splines, polycube parameterization, volumetric mapping, and computer generated line drawings. More information about his research can be found at http://www.ntu.edu.sg/home/yhe.

Dayong Wang received the Bachelor degree in Computer Science from Tsinghua University, Beijing, China in 2008. Now he is pursuing the Ph.D. degree in computer science and engineering from Nanyang University, Singapore, under the supervision of Dr. Steven C.H. Hoi and Dr. Ying He. His research interests include statistical machine learning, multimedia retrieval, and computer vision.

Steven C. H. Hoi received the Bachelor degree in computer science from Tsinghua University, Beijing, China, and his Master and Ph.D. degrees in computer science and engineering from Chinese University of Hong Kong.

He is currently an Assistant Professor in the School of Computer Engineering of Nanyang Technological University, Singapore. His research interests include statistical machine learning, multimedia information retrieval, Web search and data mining. He is a member of IEEE and ACM.